frontiers | Frontiers in Marine Science

TYPE Original Research
PUBLISHED 22 January 2025
DOI 10.3389/fmars.2024.1521036

OPEN ACCESS

EDITED BY
Sudheesh Valliyodan,
Central University of Kerala, India

REVIEWED BY
Peng Zhang,
Guangdong Ocean University, China
Regan Nicholaus,
Mbeya University of Science and Technology, Tanzania

*CORRESPONDENCE
Jae Seong Lee
leejs@kiost.ac.kr

RECEIVED 01 November 2024
ACCEPTED 26 December 2024
PUBLISHED 22 January 2025

CITATION
An S-U, Kim K-T, Kim S-H, Baek J-W, Jeong H-J, Sun C-I, Choi JY, Hong S, Lee DI and Lee JS (2025) Biogeochemical cycling of sedimentary organic carbon and benthic nutrient fluxes in the semi-enclosed Jinhae Bay, Korea: insights into benthic-pelagic coupling.
Front. Mar. Sci. 11:1521036.
doi: 10.3389/fmars.2024.1521036

Biogeochemical cycling of sedimentary organic carbon and benthic nutrient fluxes in the semi-enclosed Jinhae Bay, Korea: insights into benthic-pelagic coupling

Sung-Uk An[1,2], Kyung-Tae Kim[1], Sung-Han Kim[1,3], Ju-Wook Baek[1,3], Hyun-Jeong Jeong[1,3], Chul-In Sun[4], Jin Young Choi[1,3], Sokjin Hong[5], Dae In Lee[5] and Jae Seong Lee[1,3]*

[1]Marine Environment Research Center, Korea Institute of Ocean Science and Technology, Busan, Republic of Korea, [2]Department of Ecology and Conservation, National Marine Biodiversity Institute of Korea, Seocheon, Republic of Korea, [3]Department of Convergence Study on the Ocean Science and Technology, Ocean Science and Technology School, Busan, Republic of Korea, [4]Marine Environment Monitoring Team, Korea Marine Environment Management Corporation, Busan, Republic of Korea, [5]Marine Environment Research Division, National Institute of Fisheries Science (NIFS), Busan, Republic of Korea

The mineralization of organic matter at the sediment plays a crucial role in ecosystem functioning by facilitating the biogeochemical cycling of carbon and nutrients. This process not only supports nutrient availability for primary production but also regulates the long-term storage of carbon within sediments. To understand the biogeochemical processes associated with organic matter mineralization and nutrient regeneration, we estimated total and diffusive sediment oxygen uptake rates, benthic nutrient fluxes, and organic carbon (OC) budgets at four sites in the semi-enclosed Jinhae Bay (JB). The total oxygen uptake (TOU) rates ranged from 38.4 to 49.6 mmol O_2 m^{-2} d^{-1}, and diffusive oxygen uptake (DOU) rates ranged from 12.3 $\pm$ 1.8 to 15.1 $\pm$ 1.4 mmol O_2 m^{-2} d^{-1}. The average ratio of TOU : DOU ranged from 3.12 to 3.28 over JB, which suggests significant benthic faunal activities in JB sediments. The vertical flux of organic carbon ranged from 45.5 $\pm$ 7.0 to 93.0 $\pm$ 25.3 mmol C m^{-2} d^{-1}, and mainly consisted of biodeposits associated with aquaculture activities. The burial flux into the sediment ranged from 3.96 $\pm$ 1.00 to 7.17 $\pm$ 1.64 mmol C m^{-2} d^{-1}, and burial efficiencies were 4.25 to 15.8%, which indicated that deposited organic carbon was either mineralized in surface sediment before burial or laterally transferred by resuspension. The benthic nutrient fluxes at four sites ranged from 1.50 to 2.07 mmol m^{-2} d^{-1} for nitrogen, from 0.02 to 0.05 mmol m^{-2} d^{-1} for phosphate, and from 6.72 to 9.11 mmol m^{-2} d^{-1} for silicate. The benthic nitrogen and phosphate fluxes accounted for 82.1 to 149% and 23.1

to 57.6%, respectively, of the required levels for primary production in the water column. Our results suggest that OC oxidation in the JB sediment may significantly contribute to the biogeochemical OC cycles and tight benthic–pelagic coupling associated with nutrient regeneration.

KEYWORDS

total oxygen uptake, organic carbon mineralization, benthic nutrient flux, organic carbon budget, semi-enclosed bay

1 Introduction

Although coastal zones constitute only a small fraction (~8%) of the world's oceans, they are among the most productive ecosystems and play a crucial role in providing various ecosystem services such as food resources, protection, nursery grounds for fish, and biogeochemical reactors (Alongi, 1998; Barbier et al., 2011). Among these services, coastal zones are particularly important in mediating carbon cycling and nutrient regeneration as an ecosystem connecting terrestrial and marine environments (Ramesh et al., 2015; Cloern et al., 2016). Thus, they have been recognized as more valuable ecosystems than the open ocean (Costanza et al., 1997; 2014). However, frequent environmental disturbances in coastal areas, resulting from anthropogenic activities and climate change, threaten ecosystem functions and human health. These include red tides (harmful algal blooms), and hypoxia and eutrophication (excessive nutrient inputs leading to low oxygen levels) and are generally characterized by an intense accumulation of organic matter in the sediment, ultimately leading to significant changes in coastal biogeochemical processes associated with organic carbon (OC) mineralization and nutrient regeneration (Rowe et al., 1975; Conley et al., 2007; Lee et al., 2012; Kim et al., 2021). Understanding these coastal biogeochemical processes, involving organic matter and nutrients, is essential for assessing ecological function and the impacts of disturbances.

In coastal waters, large amounts of organic matter reach the sediment and is either mineralized or permanently buried (Burdige, 2007; Arndt et al., 2013; Larowe et al., 2020). Benthic OC mineralization occurs through a variety of degradation pathways using various electron acceptors, including O_2, NO_3^-, Mn-oxides, Fe-oxides, and SO_4^{2-} (Froelich et al., 1979; Canfield et al., 1993; Hyun et al., 2017; Zhao and Zhang, 2022). In the oxic layer of sediments, aerobic respiration is the dominant degradation process with O_2 consumption. Below the oxic layer, a significant amount of O_2 is also consumed through efficient reoxidation of reduced by-products from anaerobic mineralization (Jørgensen, 1982; Jørgensen et al., 2022). Thus, sediment oxygen uptake has been commonly used as an indicator of complex OC oxidation processes (Glud, 2008; Jørgensen et al., 2022). Benthic OC mineralization processes, which degrade organic matter in sediments, release dissolved inorganic carbon and nutrients into the sediment pore water. These may be released into the water column and contribute to primary production (Ferrón et al., 2009; Lee et al., 2012; Griffiths et al., 2017; Lacoste et al., 2022). Therefore, benthic organic matter mineralization has significant implications for the global carbon and nutrient budget, as it determines the fate of organic matter entering the sediments and influences the overall carbon and nutrient balance in coastal ecosystems (Burdige, 2007; Griffiths et al., 2017; Ehrnsten et al., 2022).

Jinhae Bay (JB) is a semi-enclosed bay with a shallow water depth (< 50 m) on the southeastern coast of Korea (Kang, 1991). Unique geographical features that limit water circulation, in conjunction with massive organic matter loading from large-scale aquaculture, industrial complexes, and coastal cities, mean the area frequently experiences hypoxia, red tides, and metal pollution (Lim et al., 2006; Lee et al., 2017, 2018; Kwon et al., 2020). In particular, seasonal hypoxia in JB is detrimental to the spawning and nursing ground of aquatic resources, imposing severe damage on the aquaculture industry, including reduced levels of fishery production, disease, and frequent fish mortality (Lim et al., 2006; Hyun et al., 2013; Lee et al., 2018). Recently, mass mortality events, accounting for about 80% of the anticipated harvest, have been reported in oyster farms on the southern coast of Korea, including in JB, during the initial winter harvesting season (NIFS, 2021). When the massive organic matter associated with various disturbance in JB exported to the sediment, it will eventually impact the functioning of benthic ecosystems by promoting carbon burial and benthic remineralization.

To assess the effects of excessive disturbance in JB, several inventory studies on the physical, chemical, and biological characteristics of water columns and sediments have been conducted over the last four decades (Cho, 1979; Kang, 1991; Lim et al., 2006; Bae et al., 2017; Yoon et al., 2019). However, in these studies, limitations in the biogeochemical information relating to OC and nutrients resulted in uncertainties when estimating the complex interaction between the sediment and water column (Lee et al., 2012; Hyun et al., 2013; Lee et al., 2018). Hence, the application of benthic–pelagic coupling, associated with biogeochemical OC cycles and nutrient regeneration, has been proposed to more effectively estimate the behavior and biogeochemical processes of OC and nutrients within coastal systems. The primary goals of this study, in the semi-enclosed

coastal ecosystem of JB, were (1) to quantify sediment oxygen uptake using an autonomous *in situ* benthic lander, (2) to estimate the partitioning sedimentary OC flux and its mass budget in the sediment, and (3) to quantify the contribution of benthic nutrient fluxes to primary production in the water column via benthic–pelagic coupling.

2 Materials and methods

2.1 Study area

JB, with an area of about 640 km^2, is the largest embayment in the southeastern part of the Korean Peninsula (Figure 1). The tide in JB is semidiurnal, with a range between 0.45 m during neap tide and 1.8 m during spring tide (Kim et al., 2014). The current during spring tide is approximately 90 cm s^{-1} and about 30 cm s^{-1} during neap tide, while weak currents (< 10 cm s^{-1}) are observed in the inner bay (Kang, 1991). JB is surrounded by the cities of Jinhae, Masan, Goseong, Tongyeong, and Geoje with a combined population of more than a million people and including an enormous industrial complex (Kim et al., 2014). JB has been one of Korea's major fisheries with high productivity and about 48 km^2 of the area is used for intensive large-scale aquaculture, including oyster, mussel, sea squirt, and blood cockle farming (Lee et al., 2018). In particular, the Jinhae-Tongyeong coast, including the JB, in southeastern Korea is a major hub for oyster aquaculture, representing about 80% of the nation's total production (http://www.foc.re.kr). In addition, long water residence times and low tidal current velocities, because of the topographic features of the semi-enclosed bay, lead to deposition of biodeposits (feces and pseudo-feces) close to the aquacultural areas (Hyun et al., 2013).

2.2 Sampling

Water and sediment core sampling, and other *in situ* experiments, were carried out in December 2022 in Dangdong Bay, which is one of the several inner bays located on the western side of JB (Figure 1). Oyster (*Grassostrea gigas*) and ascidian (*Styela clava*) farming occur around the sampling area, and large quantities of oysters are harvested during November and February. The water temperature, salinity, pH, and dissolved oxygen (DO) in the water column were measured *in situ* using a calibrated multiparameter water quality meter (YSI-6600; YSI Inc., Yellow Springs, OH, USA). Water samples from the surface and bottom layer, for the measurement of dissolved inorganic nutrients, were collected using a Niskin water sampler (model 1010, General Oceanics Inc.,

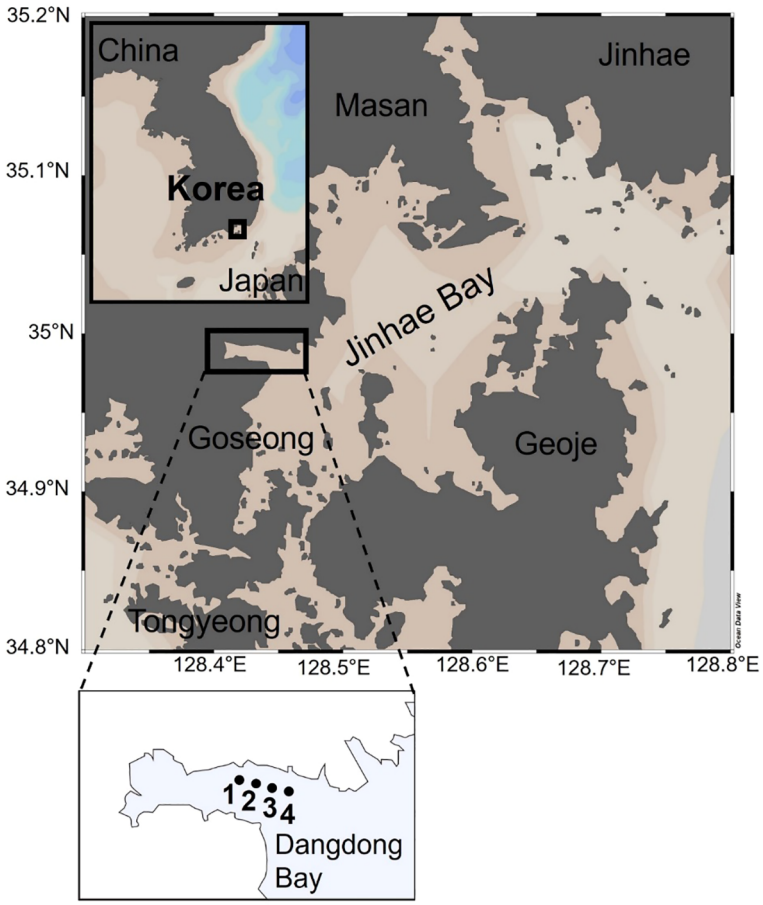

FIGURE 1
Map of the Jinhae Bay showing four sampling sites in the Dangdong Bay.

Miami Gardens, FL, USA). The water samples for measuring dissolved inorganic nutrients were immediately filtered using a membrane syringe filter (pore size: 0.45 µm, Advantec, Japan) and then stored below −20°C pending analysis.

Sediment cores for geochemical analysis were collected by scuba divers in duplicate or triplicate using an acrylic core to minimize surface disturbance. They were stored onboard in coolers with ice. Any core containing visually significant bioturbation or shells along the walls, that could affect the vertical stratifications, was not retained. Sediment pore water samples were extracted using a Rhizon sampler (Rhizon CSS, Rhizosphere Research Products, Netherlands) at 1-cm depth intervals through predrilled and taped holes in the core (Seeberg-Elverfeldt et al., 2005). Pore water samples were kept frozen (−20°C) until processed in the laboratory. Sediment samples for measuring total organic carbon (TOC) and total nitrogen (TN) content were sectioned at 0–2-cm intervals and kept in a deep freezer (−20°C) until laboratory processing.

2.3 *In situ* measurements

To estimate the *in situ* sediment total oxygen uptake (TOU) rate, diffusive oxygen uptake (DOU) rate, and benthic nutrient fluxes at the sediment–water interface, we deployed the autonomous *in situ* benthic lander on the sea floor with the assistance of a scuba diver. The benthic lander consists of the benthic chamber (Belc*II*), microprofiler (Belp*II*), and automatic water sampler (Lee et al., 2012; Cho et al., 2023). In brief, the Belc*II* contains an opaque rectangular chamber with a base area of 841 cm^2 (29 × 29 cm^2), and an automatic syringe water sampler. After reaching the seafloor and waiting for 2 h, the chambers are enclosed by a lid with a motor-driven closing system. Once the lid is closed, four stirring bars on the lid rotate at a speed of ~30 rpm, creating a diffusion boundary with a layer thickness of about 300–700 µm at the sediment–water interface (Lee et al., 2012). Variations of O_2 concentration in the chamber are measured at 10-s intervals over the incubation period by an oxygen optode sensor (4330F, Aanderaa, Norway) mounted on the lid (Lee et al., 2012; Cho et al., 2023). Meanwhile, the Belp*II* consists of the four separate O_2 microoptode systems (OXR50-HS-SUB and FSO2-SUBPORT, PyroScience GmbH, Germany) and is equipped with a custom-built motor-driven linear stage, allowing for high spatial resolution (<100 µm) measurement of oxygen at the sediment–water interface. The O_2 microoptode consists of a retractable fiber of 230 µm with a tip diameter of 50–70 µm and a 90% response time of less than 0.8 s. The zero-reading for O_2 concentration was determined in the anoxic zone of the profiles, where oxygen has reached a constant value. Before deploying the benthic lander, the oxygen sensors for the chamber were calibrated at 100% air-saturation using air-bubbled water and 0% air-saturation using sodium dithionite-added water. After bringing the benthic chamber on board, water samples were collected by syringe sampler for nutrient analysis and filtered immediately using a membrane syringe filter (pore size 0.45 µm, Advantec, Tokyo, Japan) and then stored in a freezer (−20°C) until analysis.

2.4 Sediment trap

Four acrylic cylindrical sediment traps with a diameter of 7 cm, a length of 60 cm (an aspect ratio of 8.6) were deployed for more than 24 h at each site to collect the vertical flux of particulate OC and TN (Lee et al., 2014; Kim et al., 2021; Cho et al., 2023). With the assistance of a scuba diver, these sediment traps were placed on the upper frame of the benthic lander. To ensure the preservation of particulate materials and prevent sample wash-out, the trap bottles filled with filtered saline water (more than 50) and attached to the bottom of each sediment trap after approximately 2 hours. A scuba diver subsequently recovered the sediment traps prior to retrieval of the benthic chamber. The overlying water was cautiously siphoned off within 3 h, and samples were stored in a refrigerator until laboratory processing.

2.5 Laboratory analysis

Dissolved inorganic nutrient (NH_4^+, NO_x, PO_4^{3-}, and $Si(OH)_4$) concentrations in the water column and sediment pore water were measured using an autoanalyzer (QuAAtro 39, SEAL Analytical, Mequon, WI, USA) within a week. To minimize potential artifacts for nutrient analysis, our samples were promptly thawed and filtered to remove particulate matter, ensuring that any silicate precipitate formed during freezing was excluded from analysis. Certified reference material (KANSO Ltd., Japan) was included in each batch of nutrient samples and were used to ensure the accuracy of the samples. Reproducibility was generally within ±7%. The porosity of the sediment was determined from the net weight difference between wet and dry sediment. The total organic carbon (TOC) and total nitrogen (TN) sediment contents were measured using a CHN analyzer (Thermo Finnigan Flash EA 1112) after acidification with 1 M HCl to remove $CaCO_3$. TOC and TN contents were calculated from raw data using calibration series obtained with sulfanilamide standards ($C_6H_8N_2O_2S$, Thermo Fisher Scientific Inc, USA). To estimate the vertical flux of total mass (TM), TOC, and TN, two aliquots of samples from the sediment trap were filtered through precombusted GF/F filters (6827-1315, Whatman, UK) and freeze-dried until reaching a constant weight. The filtered sample was acidified, and its TOC and TN contents were determined using the same process as for the sediment samples.

The ^{210}Pb activity in the core samples was measured using an alpha spectrometer equipped with low-background silicon-surface barrier detectors (PIPS Detector Canberra, USA) (Lee et al., 2012). This assumed that the total activity of ^{210}Po (daughter nuclide of ^{210}Pb) in the sediments had reached radioactive equilibrium with ^{210}Pb. For this measurement, about 0.5–1 g of powdered sediment was spiked with ^{209}Po and then digested with a mixture of concentrated HNO_3 and HCl on a hot plate. After reducing the ferric ions with ascorbic acid in an acid solution, the Po isotopes (^{209}Po and ^{210}Po) were spontaneously deposited onto a silver disk at 70°C for 6 h with stirring. The activity was counted over a day to obtain sufficient counts (> 1000). Excess ^{210}Pb ($^{210}Pb_{xs}$) was

determined by subtracting average ^{210}Pb activity in the lower sediment layer from the measured ^{210}Pb activities.

2.6 Flux calculations

The TOU and BNF (benthic nutrient flux) across the sediment–water interface (SWI) were calculated as:

$$F = \frac{dC}{dt} \times \frac{V}{A}$$

where F is the TOU or the BNF (mmol m^{-2} d^{-1}), dC/dt is the slope of the line derived from regressing the TOU or BNF concentration as a function of incubation time (mmol L^{-1} d^{-1}), V/A is the chamber height [V: chamber volume (m^3), A: chamber area (m^2)].

The high resolution O_2 vertical profiles at the upper diffusive boundary layer (DBL) and SWI were determined to calculate the DOU rate (Jørgensen and Revsbech, 1985). The DOU rate was derived from the *in situ* diffusion coefficient of temperature and salinity and the oxygen gradient within the DBL using the following equation (Glud, 2008):

$$DOU = -D_0 \frac{dO_2}{dz}$$

where D_0 is the molecular diffusion coefficient of oxygen corrected using *in situ* temperature and salinity (Broecker and Peng, 1974; Li and Gregory, 1974) and dO_2/dz is the oxygen concentration gradient (mmol cm^{-4}) within the DBL.

2.7 Sedimentation rate

Using the vertical $^{210}Pb_{xs}$ profiles, and assuming a steady state, the apparent sedimentation rate (SR) was estimated using:

$$A = A_0 exp[(-\frac{\lambda}{SR})z]$$

where A is the $^{210}Pb_{xs}$ activity in each sediment layer, A_0 is the $^{210}Pb_{xs}$ activity in the surface sediment (z=0), λ is the ^{210}Pb decay constant (0.031 y^{-1}), and SR is the sedimentation rate (cm y^{-1}). SR was estimated as the slope of the least-square regression between ln ($^{210}Pb_{xs}$) and sediment depth (z, cm) below the mixed surface layer of sediment.

We calculated the theoretical maximum sedimentation rate (Max_{sed}) to assess the influence of resuspended particles using the following equation (Lee et al., 2014):

$$Max_{sed} = TM/(1-\phi)\rho$$

where Max_{sed} is the maximum sedimentation rate (cm y^{-1}), the TM is the total mass flux collected by the sediment trap (g m^{-2} d^{-1}), ϕ is the surface sediment porosity, and ρ is the dry bulk density (g cm^{-3}).

2.8 Statistical analysis

Analysis of variance (ANOVA) was performed using SPSS version 21 (SPSS for windows, SPSS INC., Chicago, USA). One-way ANOVA followed by Tukey's multiple comparison or Kruskal-Wallis non-parametric multiple comparison tests were performed to assess spatial difference in the TOC and TN concentration of the sediment.

3 Results

3.1 Water column physiochemical characteristics and nutrient concentrations

The water depth, temperature, salinity, DO, and nutrients of the water samples are listed in Table 1. The water depth at the stations was approximately 15 m. Across the entire sampling site, water temperature, salinity, and pH ranged from 10.3 to 11.2°C (average, 10.8 ± 0.32°C), from 33.2 to 33.5 (average, 33.4 ± 0.09), and from

TABLE 1 Environmental parameters in the surface and bottom water at the four sampling sites.

		Temp.	Salinity	pH	DO	NH_4^+	NO_x	PO_4^{3-}	$Si(OH)_4$
		(°C)			(μmol L^{-1})				
St.1	S	11.2	33.2	7.87	290 (104)	1.89 ± 0.01	2.66 ± 0.98	0.39 ± 0.01	13.6 ± 0.17
	B	10.7	33.3	7.68	273 (97)	1.38 ± 0.05	1.51 ± 0.01	0.38 ± 0.01	14.0 ± 0.03
St.2	S	11.1	33.3	7.78	302 (96)	1.89 ± 0.01	2.04 ± 0.09	0.43 ± 0.01	14.0 ± 0.11
	B	10.6	33.5	7.81	288 (102)	1.95 ± 0.01	2.11 ± 0.09	0.37 ± 0.01	16.4 ± 0.14
St.3	S	11.0	33.3	7.66	270 (97)	1.44 ± 0.03	1.66 ± 0.01	0.41 ± 0.01	13.0 ± 0.07
	B	10.3	33.4	7.69	275 (97)	1.72 ± 0.11	1.56 ± 0.03	0.36 ± 0.00	13.9 ± 0.01
St.4	S	11.0	33.4	7.92	302 (108)	1.56 ± 0.09	1.17 ± 0.04	0.31 ± 0.01	11.5 ± 0.01
	B	10.5	33.4	7.83	281 (100)	1.71 ± 0.01	1.56 ± 0.03	0.36 ± 0.01	12.0 ± 0.02

Dissolved oxygen (DO) values within parentheses are oxygen saturation (in %).

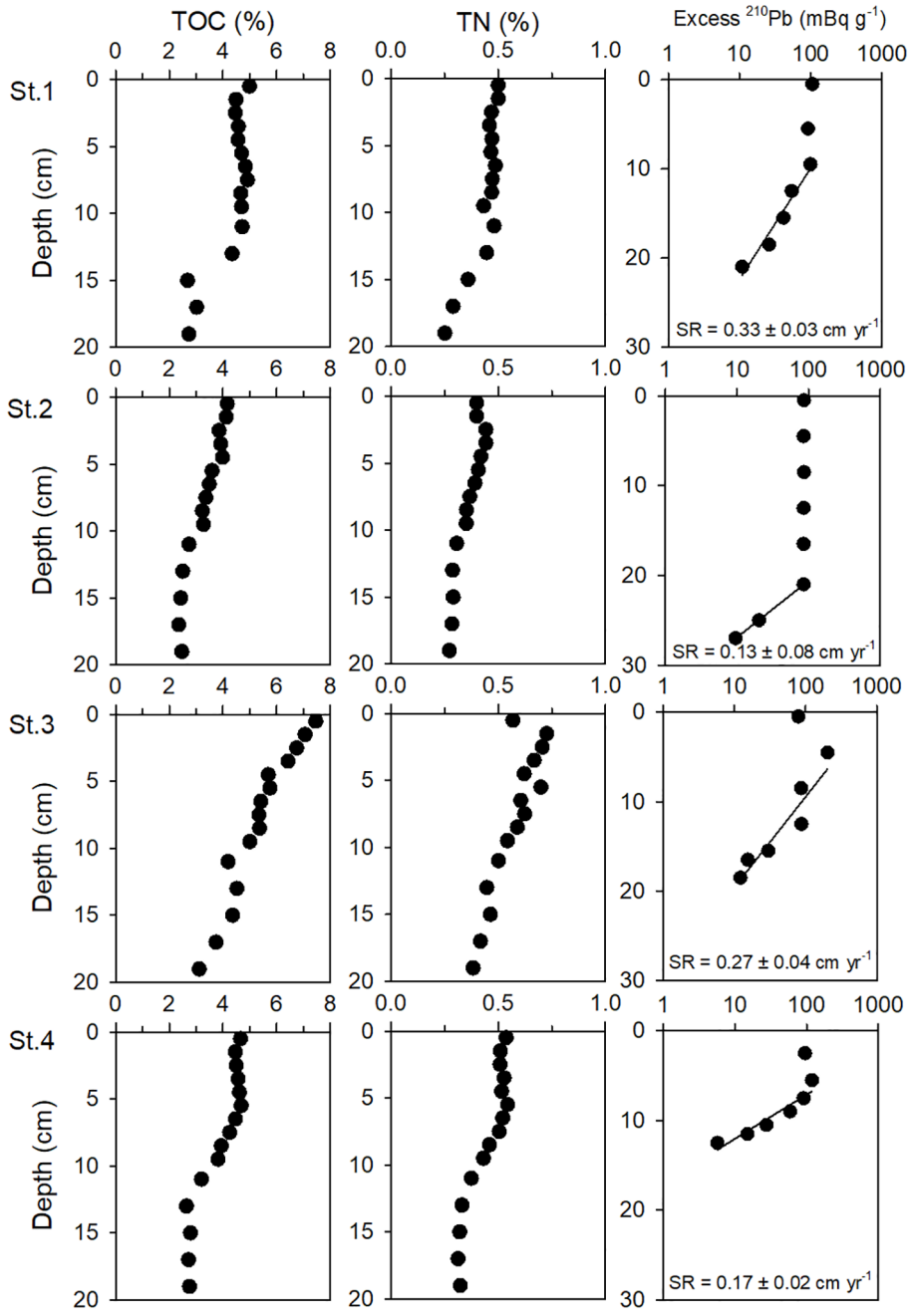

FIGURE 2
Vertical profiles of total organic carbon (TOC) and total nitrogen (TN) content in sediments at the sampling sites. The lines in the excess ^{210}Pb plot represent the linear regression fit from the relationship between activity ln(excess ^{210}Pb) and sediment depth.

7.66 to 7.92 (average, 7.78 ± 0.10), respectively. Neither temperature nor salinity exhibited significant differences horizontally or vertically, suggesting a well-mixed water column in the study area. DO concentrations ranged from 270 to 302 μmol L^{-1} (average, 285 ± 12.5 μmol L^{-1}) and were well saturated (96–108%). NH_4^+, NO_x, PO_4^{3-}, and $Si(OH)_4$ concentrations ranged from 1.38 to 1.95 μmol L^{-1} (average, 1.69 ± 0.22 μmol L^{-1}), from 1.17 to 2.66 μmol L^{-1} (average, 1.78 ± 0.46 μmol L^{-1}), from 0.31 to 0.43 μmol L^{-1} (average, 0.38 ± 0.04 μmol L^{-1}), and from 11.5 to 16.4 μmol L^{-1} (average, 13.5 ± 1.54 μmol L^{-1}), respectively.

3.2 Vertical distribution of TOC and TN

The depth profiles of TOC and TN contents in sediment at the study site are shown in Figure 2. The TOC contents in the surface sediment (< 2 cm) at St.3 were 7.26 ± 0.28%, significantly higher than those measured at St.1 (4.47 ± 0.36%), St.2 (4.14 ± 0.03%), and St.4 (4.56 ± 0.14%) (ANOVA, $p < 0.05$). Similarly, the TN content observed at St.3 (0.65 ± 0.11%) was high compared with St.1 (0.50 ± 0.001%), St.2 (0.40 ± 0.001%), and St.4 (0.52 ± 0.02%). Overall, the vertical profiles of the TOC and

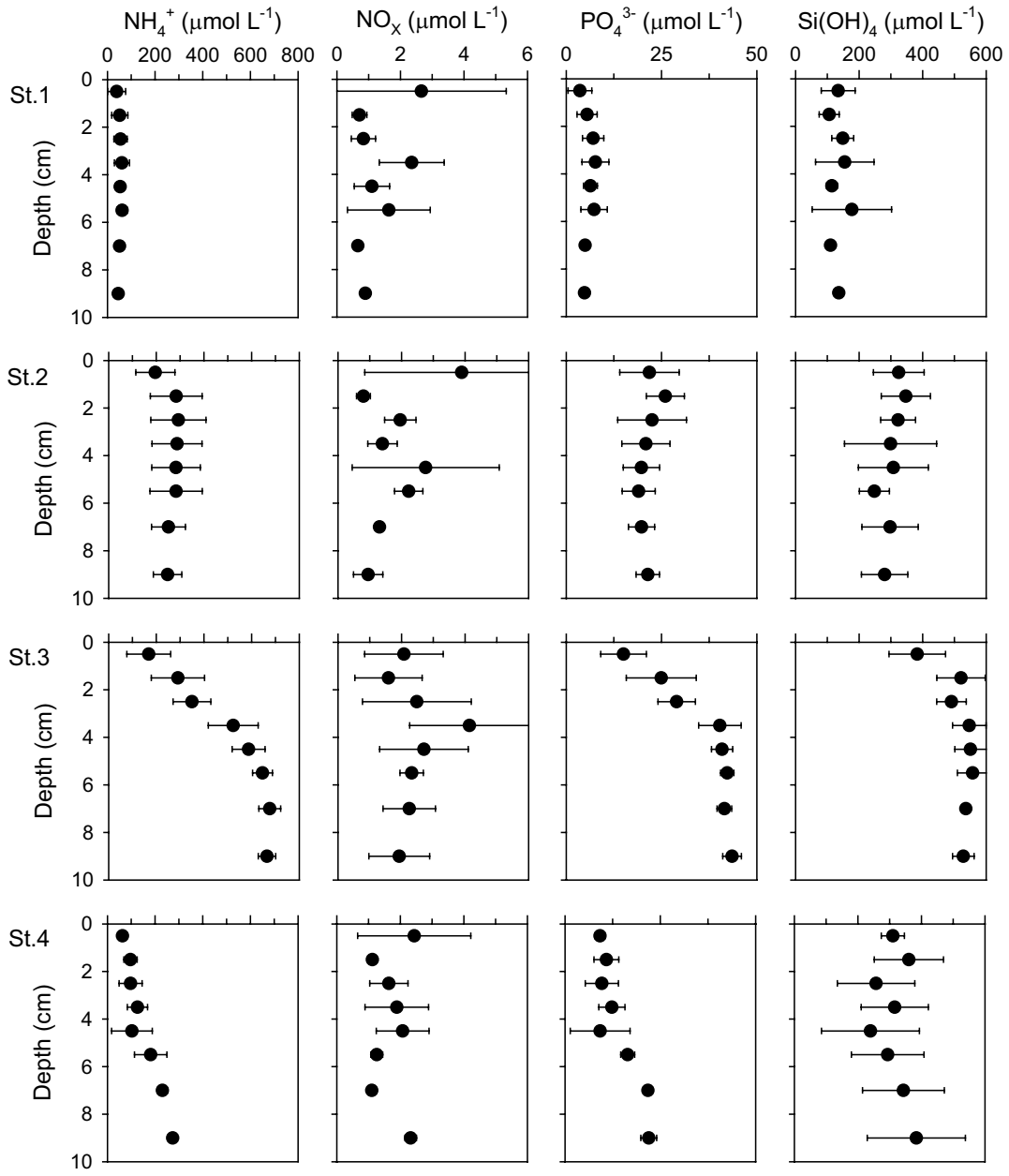

FIGURE 3
Vertical distributions of NH_4^+, NO_x, PO_4^{3-} and $Si(OH)_4$ in pore-water of the sampling sites. Error bars indicate a mean ± 1 SD from duplicate or triplicate cores.

TN contents showed a slight decrease with depth, but the profiles at St.3 showed an exceptionally steep decrease with depth (ANOVA, $p < 0.05$).

3.3 Vertical distribution of inorganic nutrients in pore water

The vertical distributions of NH_4^+, NO_x, PO_4^{3-}, and $Si(OH)_4$ concentrations in pore water are illustrated in Figure 3. NH_4^+ concentrations at St.1 remained low throughout the depth range, whereas they increased steeply in the range 0–6 cm but remained relatively constant at lower depths at St.3. NH_4^+ concentration at St.2 slightly increased near the surface, and stayed constant below, and increased slightly with depth at St.4. The highest concentrations of NO_x were measured between 0 and 1 cm at all sites, except for St.3, and the concentration decreased below 1 μmol L^{-1} at greater depths, indicative of denitrification and/or anammox processes. PO_4^{3-} and $Si(OH)_4$ in the pore water had similar vertical distribution patterns to the NH_4^+ concentrations.

10.3389/fmars.2024.1521036

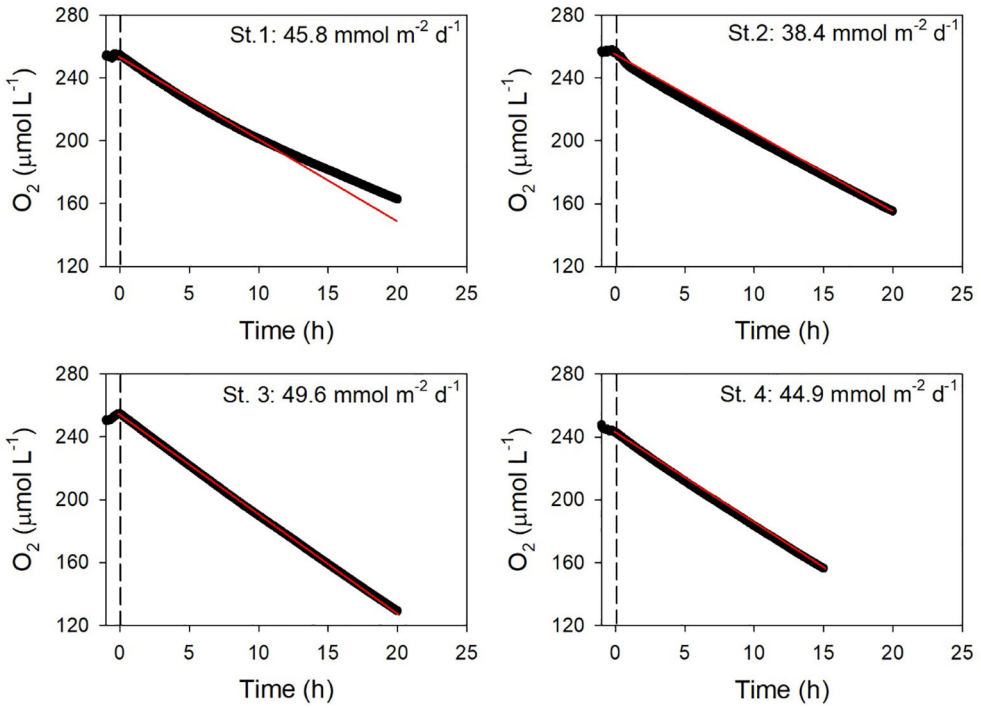

FIGURE 4
Variation of O_2 concentrations by time in the benthic chamber at the sampling sites. The red line represents the linear regression fit.

3.4 *In situ* TOU and DOU

The temporal evolution of O_2 in the benthic chamber is illustrated in Figure 4. Over time, there is a notable decrease in O_2 concentration, attributed to benthic mineralization of organic matter within the sediment. The TOU was estimated to be within the range of 38.4 to 49.6 mmol m^{-2} d^{-1} based on the gradient (dO_2/dt) of the relationship between O_2 concentration and time, as detailed in Table 2.

The vertical distributions of O_2 in the pore water at St.2, St.3, and St.4 are presented in Figure 5, measured using an *in situ* microprofiler (Belp*II*). Unfortunately, O_2 profiles at St.1 could not be obtained because the oxygen sensor's height at the time of microprofiler installation was insufficient to penetrate from the DBL to the sediment. The mean oxygen penetration depths (n = 10) at St.2, St.3, and St.4 were 3.38 ± 1.33, 2.93 ± 1.70, and 8.49 ± 4.83 mm, respectively. DOU values, estimated using the oxygen slope within the DBL, ranged from 12.3 ± 1.8 to 15.1 ± 1.4 mmol m^{-2} d^{-1} (Table 2).

3.5 Benthic nutrient flux

The nutrient concentrations in the benthic chamber generally increased during the *in situ* incubation period, but decreases in NO_x at St.2, St.3, and St.4 imply that denitrification and anammox processes might significantly influence nitrogen cycling in JB sediments (Figure 6). It remains uncertain if this phenomenon is related, but NH_4^+ benthic flux at St.1 showed a minimum. BNF estimates were based on the linear relationships between nutrient concentration and time (Figure 6). The BNF across the SWI ranged from 0.96 ± 0.04 to 2.28 ± 0.16 mmol m^{-2} d^{-1} for NH_4^+, from –0.51 ± 0.28 to 0.18 ± 0.03 mmol m^{-2} d^{-1} for NO_x, from 0.02 ± 0.01 to 0.05 ± 0.04 mmol m^{-2} d^{-1} for PO_4^{3-}, and from 6.72 ± 0.14 to 9.11 ± 0.14 mmol m^{-2} d^{-1} for $Si(OH)_4$.

TABLE 2 Total oxygen uptake (TOU), diffusive oxygen uptake (DOU), and benthic nutrient fluxes.

	TOU	DOU	NH_4^+	NO_x	PO_4^{3-}	$Si(OH)_4$
	(mmol m^{-2} d^{-1})					
St.1	45.8	–	0.96 ± 0.04	0.18 ± 0.03	0.05 ± 0.01	6.72 ± 0.14
St.2	38.4	12.3 ± 1.8	2.28 ± 0.16	-0.21 ± 0.01	0.05 ± 0.03	7.92 ± 2.21
St.3	49.6	15.1 ± 1.4	2.01 ± 0.23	-0.51 ± 0.28	0.05 ± 0.04	7.84 ± 1.81
St.4	44.9	13.7 ± 2.0	1.88 ± 0.07	-0.02 ± 0.02	0.02 ± 0.01	9.11 ± 0.14

10.3389/fmars.2024.1521036

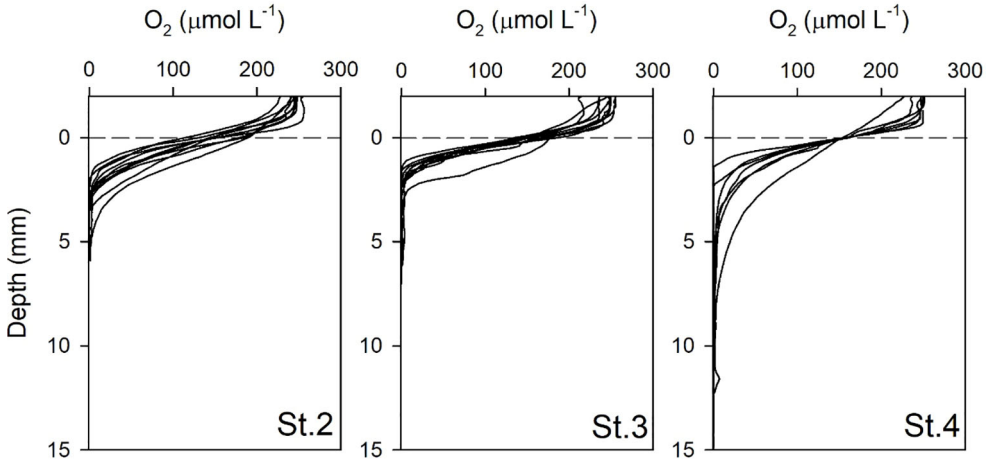

FIGURE 5
Vertical distribution of dissolved oxygen measured using a microoptode sensor with 100 μm resolution at the sampling sites.

3.6 Sedimentation rates and vertical fluxes of materials

The vertical profiles of excess ^{210}Pb in the sediment showed intensive biological mixing to a depth of 20 cm (Figure 2). The surface mixed layer at St.2 was significantly deeper than at other stations. In the vertical profiles of St.3 and St.4, the equilibrium state of ^{210}Pb was found at sediment depths deeper than 15 cm. We used average ^{210}Pb activities at equilibrium with ^{226}Ra, which showed constant activity in deeper sediment layers, to calculate the excess

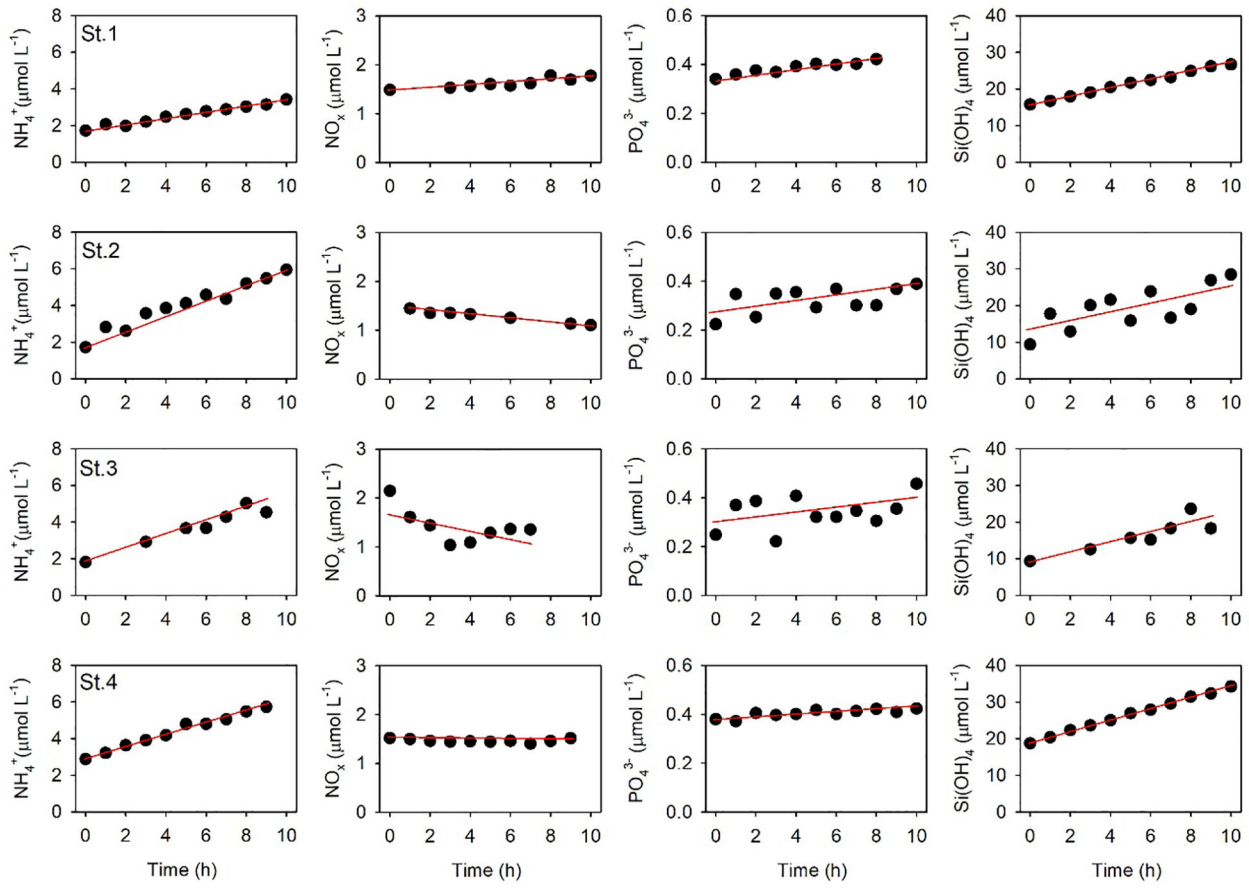

FIGURE 6
Variations of nutrient concentrations by time in the benthic chamber at the sampling sites. The red line represents the linear regression fit.

10.3389/fmars.2024.1521036

TABLE 3 Sedimentation rates (SR), vertical fluxes of total mass (TM), organic carbon (OC_{in}), and nitrogen (Nin) for using trap, primary production (PP), organic carbon lateral flux and biodeposits ($OC_{lat+bio}$), oxidation flux (OC_{ox}), burial flux (OC_{burial}), and burial efficiency.

	SR	TM	OC_{in}	N_{in}	PP	$OC_{lat+bio}$	OC_{ox}	OC_{burial}	[a]Burialefficiency
	($cm\ y^{-1}$)	($g\ m^{-2}\ d^{-1}$)	($mmol\ m^{-2}\ d^{-1}$)						(%)
St.1	0.33 ± 0.03	14.3 ± 2.90	52.1 ± 15.0	4.8 ± 1.2	9.2	42.9	35.2 ± 0.52	6.33 ± 0.78	12.2
St.2	0.13 ± 0.03	27.4 ± 5.90	93.0 ± 25.3	9.3 ± 3.9	9.2	83.8	29.5 ± 2.63	3.96 ± 1.00	4.25
St.3	0.27 ± 0.06	7.10 ± 0.80	45.5 ± 7.00	4.5 ± 0.5	9.2	36.3	38.1 ± 4.59	7.17 ± 1.64	15.8
St.4	0.17 ± 0.07	7.20 ± 0.50	50.1 ± 5.10	4.8 ± 0.5	9.2	40.9	34.5 ± 3.75	6.16 ± 2.79	12.3

a. Burial efficiency = OC_{burial}/OC_{in} x 100.

^{210}Pb activities. However, this equilibrium was not evident at St.1 and St.2 because the sediment cores collected at these stations were not long enough. Therefore, for St.1 and St.2, we used the ^{210}Pb activities at the deepest sediment layers available, at 23 cm for St.1 and 29 cm for St.2, where secular equilibrium with ^{226}Ra was assumed. The sedimentation rates, calculated from the relationship between $^{210}Pb_{xs}$ and sediment depth, were estimated to be 0.33 ± 0.03 cm y^{-1} at St.1, 0.13 ± 0.03 cm y^{-1} at St.2, 0.27 ± 0.06 cm y^{-1} at St.3, and 0.17 ± 0.07 cm y^{-1} at St.4 (Table 3).

The vertical flux of total mass (TM) ranged from 7.10 ± 0.80 to 27.4 ± 5.90 g m^{-2} d^{-1}, with the highest values at St.2 (Table 3). Vertical fluxes of OC (C_{in}) and nitrogen (N_{in}) were estimated to range from 45.5 ± 7.00 to 93.0 ± 25.3 mmol C m^{-2} d^{-1} and from 4.50 ± 0.50 to 9.30 ± 3.90 mmol N m^{-2} d^{-1}, respectively, with the maximum values observed at St.2 (Table 3).

4 Discussion

4.1 Organic carbon oxidation in the sediment

TOU has been used as the proxy for the total carbon mineralization rate in marine sediment as it encompasses both aerobic respiration and the reoxidation of reduced inorganic constituents (such as NH_4^+, Mn^{2+}, Fe^{2+}, and H_2S) from the anaerobically mediated OC degradation (Canfield et al., 2006; Glud, 2008). The estimation of OC mineralization through oxygen uptake relies on the premise that oxygen consumption directly correlates with the total carbon oxidized via aerobic and anaerobic pathways (Canfield et al., 1993). The OC oxidation rate (OC_{ox}) in the sediment was thus calculated from the TOU measurements, applying the Redfield stoichiometric ratio (C:O_2, 106:138, Redfield et al., 1963). The sedimentary OC_{ox} ranged from 29.5 ± 2.63 to 38.1 ± 4.59 mmol C m^{-2} d^{-1} (average; 34.3 mmol C m^{-2} d^{-1}) and did not exhibit distinctive spatial differences (Table 3). These ranges are lower than previous results of sea squirt and oyster farm (47–79 mmol C m^{-2} d^{-1}, Lee et al., 2011), fish farm (52.2 mmol C m^{-2} d^{-1}, Choi et al., 2020; 59.1–64.5 mmol C m^{-2} d^{-1}, Kim et al., 2021), and those are higher than shellfish farm (20.6 mmol C m^{-2} d^{-1}, Giles et al., 2006). In JB, the average ratio of OC_{DIC}, calculated from alkalinity and total dissolved inorganic carbon (DIC) flux, to OC_{ox} was 1.2, which suggests that anaerobic OC mineralization contributes to total OC oxidation (Lee et al., 2012). In addition, ratios > 1 in coastal sediments with higher organic contents indicate that a significant portion of the reduced substances are being released from the sediment layer into the bottom water or precipitated (e.g., FeS) with other reductants before undergoing complete oxidation in the oxic zone (Canfield et al., 2006; Ferrón et al., 2009). Considering that highly reduced substrates (e.g., H_2S, FeS, FeS_2) have been identified in the sediment (An, unpublished data), our estimations of OC oxidation, using TOU values and the Redfield ratio, are likely underestimated.

In general, TOU represents the sum of the DOU and benthic fauna-mediated O_2 uptake because DOU is a measure of the diffusive O_2 uptake via the sediment–water interface, excluding the impact of benthic fauna activities (Glud et al., 2003; Glud, 2008; Hicks et al., 2017; Kim et al., 2020b). In our results, the average ratio of TOU : DOU ranged from 3.12 to 3.28, which suggests significant benthic fauna activities in the JB sediments. The ratios estimated by the present study were higher than those reported in other hypoxic

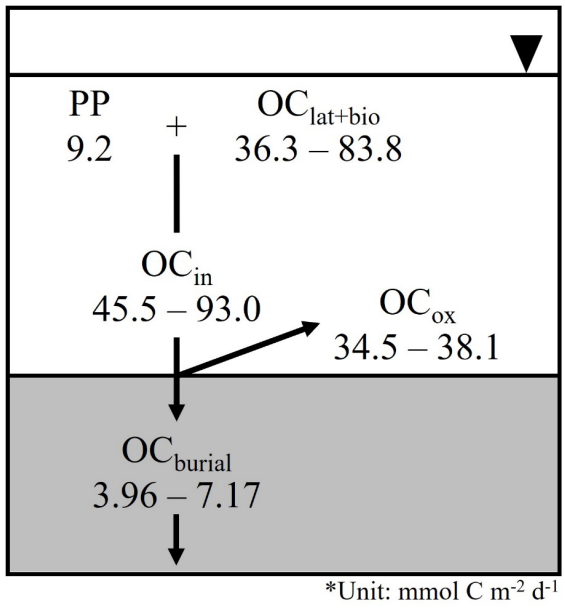

FIGURE 7
Simple organic carbon mass budget at the sampling sites. PP; primary production, $OC_{lat+bio}$; latertal transport of OC and biodeposition, OC_{in}; input flux of OC, OC_{ox}; oxidation of OC, OC_{burial}; burial flux of OC.

TABLE 4 Nutrient demand for primary production (PP) in the water column, benthic nutrient fluxes, and contribution of benthic nutrient fluxes to primary production.

Sites	Nutrient demand for PP[1]		Benthic nutrient flux		Contribution of BNFs to PP	
	(mmol m^{-2} d^{-1})		(mmol m^{-2} d^{-1})		%	
	DIN	DIP	DIN	DIP	DIN	DIP
St.1	1.39	0.09	1.14	0.05	82.1	57.6
St.2			2.07	0.05	149	57.6
St.3			1.50	0.05	108	57.6
St.4			1.90	0.02	137	23.1

[1] Calculated from the PP data from NIFS (2023) based on Redfield's ratio of C:N:P = 106:16:1.

estuary (1.14–1.90, Bonaglia et al., 2014; 1.22–1.36; Seitaj et al., 2017), semi-enclosed bay (average 1.27, Glud et al., 2003), fish farm (0.9–1.7, Cathalot et al., 2012), shallow continental shelf (average 1.42, Lansard et al., 2008; 0.94–2.82, Kim et al., 2020b), and were comparable to those of a continental shelf and slope (0.78–4.25, Archer and Devol, 1992). Indeed, the deeper surface mixed layer in the sediment may indicate intensive biological activity (Figure 2). Benthic fauna activities, including respiration, biological pumping, and bioirrigation, can significantly increase the TOU of coastal sediment (Glud et al., 2003; Glud, 2008). It can also result from increased reoxidation of reduced products from anaerobic respiration mediated by microbes, which can enhance the benthic O_2 uptake (Kristensen and Alongi, 2006; Kim et al., 2020b). Severe hypoxia has led to significant mass mortality and delayed recolonization of benthic species during the JB summer (Lim et al., 2006). However, the benthic community recovers from summer hypoxia and continues to do so until the following spring. Therefore, fauna activities associated with benthic O_2 uptake in the JB sediment during winter play an important role in the biogeochemical functioning of the benthic habitat.

4.2 Mass budget of sedimentary organic carbon

To elaborate on the driving factors affecting particulate OC in the JB sediments, we estimated the OC mass budget at each station (Figure 7). Assuming a steady state, the OC mass budget in the surface sediment layer equalizes input with outputs according to the following equation (Martens and Klump, 1984):

$$OC_{in} = OC_{ox} + OC_{burial}$$

where OC_{in} is the input flux of OC into sediment from the water column, OC_{ox} is the flux of oxidation of OC in the sediment, and OC_{burial} is the burial flux of OC into the deep sediment layer. Lateral transport and biodeposition are the dominant input fluxes of OC in JB (Lee et al., 2012; Hyun et al., 2013). To facilitate the calculation of OC mass budget, the OC produced by primary production (PP) is assumed to be deposited onto surface sediment in shallow water. Therefore, the difference between OC_{in} and PP can be represented as the sum of lateral transport of OC and/or biodeposition from aquaculture activities ($OC_{lat+bio}$). Thus, the net of OC_{in} and PP may equate to the combined ambient lateral transport of OC and biodeposition ($OC_{lat+bio}$). The PP rate in the JB water column has been estimated to be 9.2 mmol C m^{-2} d^{-1} (NIFS, 2023). The $OC_{lat+bio}$ ranged from 36.3 to 42.9 mmol C m^{-2} d^{-1} (average 40.0 ± 3.38 mmol C m^{-2} d^{-1}), which is significantly higher than the PP in the water column. In JB, the aquaculture sector is mainly in the inner bay area and accounts for almost two-thirds of the commercial oyster and ascidian aquaculture in Korea (http://www.foc.re.kr). The aquaculture of filter-feeding shellfish (ex., oyster, mussel, and clam) and ascidian (*S. clava*) generates massive biodeposit volumes composed of pseudo-feces and feces that are enriched with organic content (Fiala-Médioni, 1974; Callier et al., 2006; Mitchell, 2006; Xia et al., 2019). In addition, the long-lines, net cages, and aquaculture infrastructure can change the hydrologic system and encourage the deposition of OC surrounding an aquaculture farm (Lee et al., 2011; Kim et al., 2020a). High contributions of biodeposits to OC_{in} mainly occur in and around sea squirt farms (Lee et al., 2012), mussel farms (Zúñiga et al., 2014; Lacoste et al., 2018; 2022), oyster–seaweed farms (Xia et al., 2019), and scallop farms (Zhou et al., 2006). Thus, massive biodeposits from oyster aquaculture seem to be the dominant source of OC_{in} in JB (Lee et al., 2011; Hyun et al., 2013).

The vertical fluxes collected by the sediment trap in coastal waters may be influenced by the resuspension of bottom sediments. The calculated Max_{sed} ranged from 0.42 cm y^{-1} to 2.1 cm y^{-1}, which is approximately 2 to 3 times higher than the estimated SR from the excess ^{210}Pb profiles, except for St.2, where it is 16 times higher. Considering the uncertainties of the sediment trap (Reimers and Suess, 1983), we believe that our assessment of the influence of resuspension and/or biodeposition on OC_{in} is valid.

OC_{burial} into the deep sediment layer were calculated using the SR and the mean organic carbon content (largely constant) of the lower layer (> 30 cm) by applying the equation:

$$OC_{burial} = SR\rho(1 - \phi)OC_{\infty}$$

where SR is the sedimentation rate estimated from the excess ^{210}Pb activity (cm y^{-1}), ρ is the dry bulk density of the sediment, assumed to be 2.45 g cm^{-3} (Kim et al., 2021), ϕ is the porosity, and OC_{∞} is the mean organic carbon content below the mixed layer (mmol C g^{-1}). The burial fluxes of OC in the JB sediment ranged from 3.96 ± 1.00 to 7.17 ± 1.64 mmol C m^{-2} d^{-1} (average 5.91 ± 1.37 mmol C m^{-2} d^{-1}) (Table 3). Burial efficiencies, which were calculated

as $OC_{burial}/OC_{in} \times 100$, ranged from 4.25% to 15.8% (Table 3), which is similar to, or higher than, previous results from a finfish cage farm (3.3%, Sim et al., 2023; 6–8%, Kim et al., 2021), a sea squirt farm (3.77%, Lee et al., 2012), and an oyster farm (6–10%, Kim et al., 2021). The findings indicate that a significant portion of the deposited OC was mineralized within the surface sediment layer.

The sum of OC_{ox} and OC_{burial} in JB was lower than the vertical flux of OC, which implies that OC is being transported through resuspension and deposited elsewhere. For example, OC released from aquaculture sediment can be transported and deposited over distances of tens to hundreds of meters through processes such as deposition and lateral transport (Hatcher et al., 1994; Kim et al., 2021). This laterally transported OC can also contribute to the vertical flux, influencing sedimentary OC dynamics in adjacent ecosystems (Kim et al., 2020a). The tidal current velocity in the study area was less than 10 cm s^{-1}, which is below the threshold current velocity (15–20 cm s^{-1}) required to lateral transport according to resuspended biodeposits (i.e., feces and pseudo-feces) (Widdows et al., 1998). However, a tentative threshold current velocity for reworking muds on the seabed in JB may be around 10 cm s^{-1} at 1 m above the seabed (Lee et al., 2006). In addition, JB has numerous small islands, prominent coasts, and a swiftly shifting sea floor topography, and thus, topography and ocean currents combine to create small-scale eddy circulation (Kim et al., 2024). Therefore, we suggest that the source and physico-chemical processes of OC in the sediment are likely to have affected the calculated OC mass balance and should be further investigated to understand their potential consequences.

4.3 Benthic nutrient release and benthic–pelagic coupling

The fluxes of dissolved inorganic nitrogen (DIN, $NH_4^+ + NO_x$; 1.11–2.03 mmol N m^{-2} d^{-1}) and dissolved inorganic phosphate (DIP, PO_4^{3-}; 0.02–0.05 mmol P m^{-2} d^{-1}) measured in JB were comparable with, or lower than, previous winter-time measurements at an oyster farm (5.74 mmol N m^{-2} d^{-1} and 0.32 mmol P m^{-2} d^{-1}, Lee et al., 2011; 1.3 mmol N m^{-2} d^{-1} and0.05 mmol P m^{-2} d^{-1}, Hyun et al., 2013; 8.95 mmol N m^{-2} d^{-1} and 0.51 mmol P m^{-2} d^{-1}, Kim et al., 2021), a sea squirt farm (0.92 mmol N m^{-2} d^{-1}; Lee et al., 2011), and a finfish farm (1.41 mmol N m^{-2} d^{-1} and 1.77 mmol P m^{-2} d^{-1}; Choi et al., 2020; 5.45 mmol N m^{-2} d^{-1} and 1.67 mmol P m^{-2} d^{-1}; Kim et al., 2021). In shallow coastal waters, DIN and DIP released from sediment can be an important source supporting primary production in the water column via benthic–pelagic coupling (Ferrón et al., 2009; Lee et al., 2012; Dixon et al., 2014; Choi et al., 2020). We calculated the potential contribution of benthic nutrients fluxes for primary production using the Redfield ratio (C:N:P = 106:16:1) and compared these with the apparent DIN and DIP demand for primary production of 1.39 mmol m^{-2} d^{-1} and 0.09 mmol m^{-2} d^{-1}, respectively (Table 4). In the present study, the DIN and DIP fluxes from sediment accounted for 82.1 to 149% and 23.1 to 57.6% of N and P primary production demand (Table 4). In November, benthic DIN and DIP could support 29 to 152% and 0 to 137%, respectively, of primary production at sea squirt and oyster farms in JB and Tongyeong (Lee et al., 2011). In December, benthic DIN and DIP release 23 to 270% and 40 to 804%, respectively, of the primary production demand at finfish and oyster farms and reference sites in the inner part of Geoje-Tongyeong coastal area (Kim et al., 2021). These results indicate the importance of benthic nutrient regeneration in maintaining primary production in JB.

5 Conclusion

JB is known for the eutrophicated region that surrounds urban and offshore aquaculture activities. The presumed accumulation of organic matter in the bottom sediments causes anoxic water masses to form periodically, causing mass mortality among marine life. The periods of anoxic water mass formation are gradually increasing. However, the biogeochemical cycling of OC in the sediment boundary layer is still poorly understood. Therefore, estimation of the OC mass balance in the sediment surface layer is essential for understanding the benthic environment. This study is the first to report *in situ* measurements of benthic respiration and BNF, along with sedimentary OC burial rates, in OC-enriched sediment within JB. The benthic OC oxidation rate did not show spatial differences, and the ratio of TOU/DOU suggested that fauna activities may be a key factor in benthic respiration in JB sediment. The vertical flux of OC suggested that the input of organic matter associated with biodeposition is likely driven by aquaculture activities. Burial fluxes of OC ranged from 3.96 ± 1.00 to 7.17 ± 1.64 mmol C m^{-2} d^{-1} in JB sediment. Burial efficiencies were estimated to range from 4.25% to 15.8%, similar to other coastal waters, implying that OC oxidation in the surface sediment may significantly contribute to the biogeochemical OC cycles. The N and P needs of pelagic primary productivity are predominantly sustained by the benthic flux. This implies that BNFs serve as a noteworthy source for primary productivity in JB, suggesting that JB may have tight benthic–pelagic coupling.

Data availability statement

The original contributions presented in the study are included in the article/supplementary material. Further inquiries can be directed to the corresponding author.

Author contributions

S-UA: Conceptualization, Investigation, Writing – original draft, Writing – review & editing. K-TK: Conceptualization, Writing – review & editing. S-HK: Investigation, Visualization, Writing – original draft, Writing – review & editing. J-WB: Investigation, Writing – review & editing. H-JJ: Investigation, Writing – review & editing. C-IS: Investigation, Writing – review & editing. JC: Visualization, Writing – original draft, Writing – review & editing. SH: Visualization, Writing – review & editing. DL:

Writing – original draft, Writing – review & editing. JL: Conceptualization, Investigation, Supervision, Writing – original draft, Writing – review & editing.

Funding

The author(s) declare financial support was received for the research, authorship, and/or publication of this article. This work was supported by the Korea Institute of Ocean Science and Technology (PEA0053) and the National Institute of Fisheries Science (R2025043).

Conflict of interest

Author C-IS was employed by Korea Marine Environment Management Corporation.

The remaining authors declare that the research was conducted in the absence of any commercial or financial relationships that could be construed as a potential conflict of interest.

Generative AI statement

The author(s) declare that no Generative AI was used in the creation of this manuscript.

Publisher's note

References

Alongi, D. M. (1998). *Coastal Ecosystem Processes* Vol. 419 (Boca Raton, FL: CRC Press).

Archer, R. C., and Devol, A. (1992). Benthic oxygen fluxes on the Washington shelf and slope: a comparison of *in situ* microelectrode and chamber flux measurements. *Limnol. Oceanogr.* 37, 614–629. doi: 10.4319/lo.1992.37.3.0614

Arndt, S., Jørgensen, B. B., LaRowe, D. E., Middelburg, J. J., Pancost, R. D., and Regnier, P. (2013). Quantifying the degradation of organic matter in marine sediments: A review and synthesis. *Earth Sci. Rev.* 123, 53–86. doi: 10.1016/j.earscirev.2013.02.008

Bae, H., Lee, J. H., Song, S. J., Park, J., Kwon, B. O., Hong, S., et al. (2017). Impacts of environmental and anthropogenic stresses on macrozoobenthic communities in Jinhae Bay, Korea. *Chemosphere* 171, 681–691. doi: 10.1016/j.chemosphere.2016.12.112

Barbier, E. B., Hacker, S. D., Kennedy, C., Koch, E. W., Stier, A. C., and Silliman, B. R. (2011). The value of estuarine and coastal ecosystem services. *Ecol. Monogr.* 81, 169–193. doi: 10.1890/10-1510.1

Bonaglia, S., Nascimento, F., Bartoli, M., Klawonn, I., and Brüchert, V. (2014). Meiofauna increases bacterial denitrification in marine sediments. *Nat. Commun.* 5, 5133. doi: 10.1038/ncomms6133

Broecker, W. S., and Peng, T.-H. (1974). Gas exchange rates between air and sea. *Tellus* 26 (5), 21–35. doi: 10.3402/tellusa.v26i1-2.9733

Burdige, D. J. (2007). Preservation of organic matter in marine sediments: controls, mechanisms, and an imbalance in sediment organic carbon budgets? *Chem. Rev.* 107, 467–485. doi: 10.1021/cr050347q

Callier, M. D., Weise, A. M., McKindsey, C. W., and Desrosiers, G. (2006). Sedimentation rates in a suspended mussel farm (Great-Entry Lagoon, Canada): biodeposit production and dispersion. *Mar. Ecol. Prog. Ser.* 322, 129–141. doi: 10.3354/meps322129

Canfield, D. E., Thamdrup, B., and Hansen, J. W. (1993). The anaerobic degradation of organic matter in Danish coastal sediments: iron reduction, manganese reduction, and sulfate reduction. *Geochim. Cosmochim. Acta* 57, 3867–3883. doi: 10.1016/0016-7037(93)90340-3

Canfield, D. E., Thamdrup, B., and Kristensen, E. (2006). *Aquatic Geomicrobiology* Vol. 640 (Amsterdam: Elsevier).

Cathalot, C., Lansard, B., Hall, P. O. J., Tengberg, A., Almroth-Rosell, E., Apler, A., et al. (2012). Spatial and temporal variability of benthic respiration in a scottish sea loch impacted by fish farming: a combination of *in situ* techniques. *Aquat. Geochem.* 18, 515–541. doi: 10.1007/s10498-012-9181-4

Cho, C. H. (1979). Mass mortality of oyster due to red tide in Jinhae bay in 1978. *Bull. Korean Fish. Soc* 12, 27–33.

Cho, Y.-H., Baek, J.-W., An, S.-U., Yoo, H.-J., Baek, H.-M., Choi, J. Y., et al. (2023). Benthic respiration and heavy metal benthic fluxes in artificial Shihwa Lake: approaching *in situ* measurement. *J. Mar. Sci. Eng.* 11, 2186. doi: 10.3390/jmse11112186

Choi, A., Kim, B., Mok, J.-S., Yoo, J., Kim, J. B., Lee, W.-C., et al. (2020). Impact of finfish aquaculture on biogeochemical processes in coastal ecosystems and elemental sulfur as a relevant proxy for assessing farming condition. *Mar. pollut. Bull.* 150, 110635. doi: 10.1016/j.marpolbul.2019.110635

Cloern, J. E., Abreu, P. C., Carstensen, J., Chauvaud, L., Elmgren, R., Grall, J., et al. (2016). Human activities and climate variability drive fast-paced change across the world's estuarine-coastal ecosystems. *Glob. Change Biol.* 22, 513–529. doi: 10.1111/gcb.13059

Conley, D. J., Carstensen, J., Ærtebjerg, G., Christensen, P. B., Dalsgaard, T., Hansen, J. L. S., et al. (2007). Long-term changes and impacts of hypoxia in Danish coastal waters. *Ecol. Appl.* 17, 165–184. doi: 10.1890/05-0766.1

Costanza, R., Arge, R., Groot, R., Farberk, S., Grasso, M., Hannon, B., et al. (1997). The value of the world' s ecosystem services and natural capital. *Nature* 387, 253–260. doi: 10.1038/387253a0

Costanza, R., de Groot, R., Sutton, P., van der Ploeg, S., Anderson, S. J., Kubiszewski, I., et al. (2014). Changes in the global value of ecosystem services. *Glob. Environ. Change* 26, 152–158. doi: 10.1016/j.gloenvcha.2014.04.002

Dixon, L. K., Murphy, P. J., Becker, N. M., and Charniga, C. M. (2014). The potential role of benthic nutrient flux in support of *Karenia* blooms in west Florida (USA) estuaries and the nearshore Gulf of Mexico. *Harm. Algae.* 38, 30–39. doi: 10.1016/j.hal.2014.04.005

Ehrnsten, E., Savchuk, O. P., and Gustafsson, B. G. (2022). Modelling the effects of benthic fauna on carbon, nitrogen and phosphorus dynamics in the Baltic Sea. *Biogeosciences* 19, 3337–3367. doi: 10.5194/bg-19-3337-2022

Ferrón, S., Alonso-Pérez, F., Anfuso, E., Murillo, F. J., Ortega, T., Castro, C. G., et al. (2009). Benthic nutrient recycling on the northeastern shelf of the Gulf of Cadiz (SW Iberian Peninsula). *Mar. Ecol. Prog. Ser.* 390, 79–95. doi: 10.3354/meps08199

Fiala-Médioni, A. (1974). Ethologie alimentaire d'invertébrés benthiques filtreurs (ascidies). II. Variations des taux de filtration et de digestion en fonction de l'espèce. *Mar. Biol.* 28, 199–206. doi: 10.1007/BF00387298

Froelich, P. N., Klinkhammer, G. P., Bender, M. L., Luedtke, N. A., Heath, G. R., Cullen, D., et al. (1979). Early oxidation of organic matter in pelagic sediments of the eastern equatorial Atlantic: suboxic diagenesis. *Geochim. Cosmochim. Acta* 43, 1075–1090. doi: 10.1016/0016-7037(79)90095-4

Giles, H., Pilditch, C. A., and Bell, D. G. (2006). Sedimentation from mussel (Perna canaliculus) culture in the Firth of Thames, New Zealand: Impacts on sediment oxygen and nutrient fluxes. *Aquac* 261, 125–140. doi: 10.1016/j.aquaculture.2006.06.048

Glud, R. N. (2008). Oxygen dynamics of marine sediments. *Mar. Biol. Res.* 4, 243–289. doi: 10.1080/17451000801888726

Glud, R. N., Gundersen, J. K., Røy, H., and Jørgensen, B. B. (2003). Seasonal dynamics of benthic O_2 uptake in a semienclosed bay: importance of diffusion and faunal activity. *Limnol. Oceanogr.* 48, 1265–1276. doi: 10.4319/lo.2003.48.3.1265

Griffiths, J. R., Kadin, M., Nascimento, F. J. A., Tamelander, T., Törnroos, A., Bonaglia, S., et al. (2017). The importance of benthic–pelagic coupling for marine ecosystem functioning in a changing world. *Glob. Change Biol.* 23, 2179–2196. doi: 10.1111/gcb.13642

Hyun, J.-H., Kim, S.-H., Mok, J.-S., Cho, H., Lee, T., Vandieken, V., et al. (2017). Manganese and iron reduction dominate organic carbon oxidation in surface sediments of the deep Ulleung Basin, East Sea. *Biogeosciences* 14, 941–958. doi: 10.5194/bg-14-941-2017

Hyun, J.-H., Kim, S.-H., Mok, J.-S., Lee, J. S., An, S.-U., Lee, W.-C., et al. (2013). Impacts of long-line aquaculture of Pacific oysters (*Crassostrea gigas*) on sulfate reduction and diffusive nutrient flux in the coastal sediments of Jinhae-Tongyeong, Korea. *Mar. pollut. Bull.* 74, 187–198. doi: 10.1016/j.marpolbul.2013.07.004

Hatcher, A., Grant, J., and Schofield, B. (1994). Effects of suspended mussel culture (Mytilus spp.) on sedimentation, benthic respiration and sediment nutrient dynamics in a coastal bay. *Mar. Ecol. Prog. Ser.* 115, 219–235. doi: 10.3354/meps115219

Hicks, N., Ubbara, G. R., Silburn, B., Smith, H. E. K., Kröger, S., Parker, E. R., et al. (2017). Oxygen dynamics in shelf seas sediments incorporating seasonal variability. *Biogeochemistry* 135, 35–47. doi: 10.1007/s10533-017-0326-9

Jørgensen, B. B. (1982). Mineralization of organic matter in the seabed-the role of sulphate reduction. *Nature* 96, 643–645. doi: 10.1038/296643a0

Jørgensen, B. B., and Revsbech, N. P. (1985). Diffusive boundary layers and the oxygen uptake of sediment and detritus. *Limmol. Oceanogr* 30, 111–112. doi: 10.4319/lo.1985.30.1.0111

Jørgensen, B. B., Wenzhöfer, F., Egger, M., and Glud, R. N. (2022). Sediment oxygen consumption: role in the global marine carbon cycle. *Earth Sci. Rev.* 228, 103987. doi: 10.1016/j.earscirev.2022.103987

Kang, S. W. (1991). Circulation and pollutant dispersion in Masan-Jinhae Bay of Korea. *Mar. pollut. Bull.* 23, 37–40. doi: 10.1016/0025-326X(91)90646-A

Kim, D., Baek, S. H., Yoon, D. Y., Kim, K. H., Jeong, J. H., Jang, P. G., et al. (2014). Water quality assessment at Jinhae Bay and Gwangyang Bay, South Korea. *Ocean Sci. J.* 49, 251–264. doi: 10.1007/s12601-014-0026-5

Kim, J., Choi, B.-J., Choi, J.-S., and Ha, H. K. (2024). Seasonal circulation and estuarine characteristics in the Jinhae and Masan Bay from three-dimensional numerical experiments. *Sea: J. Korean Soc Oceanogr.* 29, 77–100. doi: 10.7850/jkso.2024.29.2.077

Kim, S.-H., Kim, H. C., Choi, S.-H., Lee, W.-C., Jung, R.-H., Hyun, J.-H., et al. (2020a). Benthic respiration and nutrient release associated with net cage fish and longline oyster aquaculture in the Geoje-Tongyeong coastal waters in Korea. *Estuaries Coast.* 43, 589–601. doi: 10.1007/s12237-019-00567-5

Kim, S.-H., Lee, J.-S., Kim, K.-T., Kim, H.-C., Lee, W.-C., Choi, D., et al. (2021). Aquaculture farming effect on benthic respiration and nutrient flux in semi-enclosed coastal waters of Korea. *J. Mar. Sci. Eng.* 9, 554. doi: 10.3390/jmse9050554

Kim, S.-H., Lee, J.-S., Kim, K.-T., Kim, S.-L., Yu, O. H., Lim, D., et al. (2020b). Low benthic mineralization and nutrient fluxes in the continental shelf sediment of the northern East China Sea. *J. Sea Res.* 164, 101934. doi: 10.1016/j.seares.2020.101934

Kristensen, E., and Alongi, D. M. (2006). Control by fiddler crabs (*Uca vocans*) and plant roots (*Avicennia marina*) on carbon, iron, and sulfur biogeochemistry in mangrove sediment. *Limnol. Oceanogr.* 51, 1557–1571. doi: 10.4319/lo.2006.51.4.1557

Kwon, H. K., Kim, G., Lim, W. A., Park, J. W., and Park, T. G. (2020). Conditions of nutrients and dissolved organic matter for the outbreaks of Paralytic Shellfish Poisoning (PSP) in Jinhae Bay, Korea. *Mar. pollut. Bull.* 158, 111381. doi: 10.1016/j.marpolbul.2020.111381

Lacoste, É, Drouin, A., Weise, A. M., Archambault, P., and McKindsey, C. W. (2018). Low benthic impact of an offshore mussel farm in Îles-de-la-Madeleine, eastern Canada. *Aquac. Environ. Interact.* 10, 473–485. doi: 10.3354/aei00283

Lacoste, É., Bec, B., Le Gall, P., Boufahja, F., Raimbault, P., Messiaen, G., et al. (2022). Benthic-pelagic coupling under juvenile oyster influence in a French Mediterranean coastal lagoon (Thau Lagoon). *Estuar. Coast. Shelf. Sci.* 267, 107779. doi: 10.1016/j.ecss.2022.107779

Lansard, B., Rabouille, C., Denis, L., and Grenz, C. (2008). *In situ* oxygen uptake rates by coastal sediment under the influence of the Rhone River (NW Mediterranean Sea). *Cont. Shelf Res.* 28, 1501–1510. doi: 10.1016/j.csr.2007.10.010

Larowe, D. E., Arndt, S., Bradley, J. A., Estes, E. R., Hoarfrost, A., Lang, S. Q., et al. (2020). The fate of organic carbon in marine sediments – new insights from recent data and analysis. *Earth Sci. Rev.* 204, 103146. doi: 10.1016/j.earscirev.2020.103146

Lee, J. S., Han, J. H., An, S.-U., Na, T., Kwon, J. N., and Kim, E.-S. (2014). Sedimentary organic carbon budget of coastal sediments and the importance of benthic-pelagic coupling off Namhae Island in the South Sea of Korea. *Ocean Sci. J.* 49, 433–447. doi: 10.1007/s12601-014-0041-6

Lee, J., Kim, S.-G., and An, S. (2017). Dynamics of the physical and biogeochemical processes during hypoxia in Jinhae Bay, South Korea. *J. Coast. Res.* 33, 854–863. doi: 10.2112/JCOASTRES-D-16-00122.1

Lee, J. S., Kim, S.-H., Kim, Y.-T., Hong, S. J., Han, J. H., Hyun, J. H., et al. (2012). Influence of sea squirt (*Halocynthia roretzi*) aquaculture on benthic-pelagic coupling in coastal waters: a study of the South Sea in Korea. *Estuar. Coast. Shelf Sci.* 99, 10–20. doi: 10.1016/j.ecss.2011.11.013

Lee, J. S., Kim, Y.-T., Shin, K.-H., Hyun, J.-H., and Kim, S.-Y. (2011). Benthic nutrient fluxes at longline sea squirt and oyster aquaculture farms and their role in coastal ecosystems. *Aquacult. Int.* 19, 931–944. doi: 10.1007/s10499-010-9411-y

Lee, J., Park, K.-T., Lim, J.-H., Yoon, J.-E., and Kim, I.-N. (2018). Hypoxia in Korean coastal waters: a case study of the natural Jinhae Bay and artificial Shihwa Bay. *Front. Mar. Sci.* 5. doi: 10.3389/fmars.2018.00070

Lee, H. J., Wang, Y. P., Chu, Y. S., and Jo, H. R. (2006). Suspended sediment transport in the coastal area of Jinhae Bay–Nakdong Estuary, Korea Strait. *J. Coast. Res.* 22, 1062–1069. doi: 10.2112/04-0231.1

Li, Y.-H., and Gregory, S. (1974). Diffusion of ions in sea water and in deep-sea sediment. *Geochim. Cosmochim. Acta* 38, 703–714. doi: 10.1016/0016-7037(74)90145-8

Lim, H.-S., Diaz, R. J., Hong, J.-S., and Schaffner, L. C. (2006). Hypoxia and benthic community recovery in Korean coastal waters. *Mar. pollut. Bull.* 52, 1517–1526. doi: 10.1016/j.marpolbul.2006.05.013

Martens, C. S., and Klump, J. V. (1984). Biogeochemical cycling in an organic-rich coastal marine basin 4. An organic carbon budget for sediments dominated by sulfate reduction and methanogenesis. *Geochim. Cosmochim. Acta* 48 (10), 1987–2004. doi: 10.1016/0016-7037(84)90380-6

Mitchell, I. M. (2006). *In situ* biodeposition rates of Pacific oysters (*Crassostrea gigas*) on a marine farm in Southern Tasmania (Australia). *Aquaculture* 257, 194–203. doi: 10.1016/j.aquaculture.2005.02.061

NIFS (2023). *National Institute of Fisheries Science report on the study on sustainable fishery productivity in the northwestern area of Jinhae Bay*.

NIFS (National Institute of Fisheries Science) (2021). Available online at: https://www.nifs.go.kr/news/actionNewsList.do (Accessed December 14, 2021).

Ramesh, R., Chen, Z., Cummins, V., Day, J., D'Elia, C., Dennison, B., et al. (2015). Land-Ocean interactions in the coastal zone: past, present and future. *Anthropocene* 12, 95–98. doi: 10.1016/j.ancene.2016.01.005

Redfield, A. C., Ketchum, B. H., and Richards, F. A. (1963). "The influence of organisms on the composition of the sea water," in *The Sea*, vol. 2 . Ed. M. N. Hill (Interscience Publishers, New York), 26–77.

Reimers, C. E., and Suess, E. (1983). The partitioning of organic carbon fluxes and sedimentary organic matter decomposition rates in the ocean. *Mar. Chem.* 13, 141–168. doi: 10.1016/0304-4203(83)90022-1

Rowe, G. T., Clifford, C. H., and Smith, K. L.Jr. (1975). Benthic nutrient regeneration and its coupling to primary productivity in coastal waters. *Nature* 255, 215–217. doi: 10.1038/255215a0

Seeberg-Elverfeldt, J., Schluter, M., Feseker, T., and Kölling, M. (2005). Rhizon sampling of porewaters near the sediment-water interface of aquatic systems. *Limnol. Oceanogr.-Methods.* 3, 361–371. doi: 10.4319/lom.2005.3.361

Seitaj, D., Sulu-Gambari, F., Burdorf, L. D. W., RomeroRamirez, A., Maire, O., Malkin, S. Y., et al. (2017). Sedimentary oxygen dynamics in a seasonally hypoxic basin, *Limnol. Oceanogr* 62, 452–473. doi: 10.1002/lno.10434

Sim, B., Kim, H. C., Yoon, S., Hong, S., Jung, W., and Kang, S. (2023). Mass balance of finfish cage farm in South Korea. *Korean J. Fish Aquat. Sci.* 56, 473–483.

Widdows, J., Brinsley, M. D., Bowley, N., and Barrett, C. (1998). A benthic annular flume for *in situ* measurement of suspension feeding/biodeposition rates and erosion potential of intertidal cohesive sediments. *Estuar. Coast. Shelf Sci.* 46, 27–38. doi: 10.1006/ecss.1997.0259

Xia, B., Han, Q., Chen, B., Sui, Q., Jiang, T., Sun, X., et al. (2019). Influence of shellfish biodeposition on coastal sedimentary organic matter: a case study from Sanggou Bay, China. *Cont. Shelf Res.* 172, 12–21. doi: 10.1016/j.csr.2018.11.002

Yoon, J.-E., Lim, J.-H., Son, S., Youn, S.-H., Oh, H.-J., Hwang, J.-D., et al. (2019). Assessment of satellite-based Chlorophyll-a algorithms in eutrophic Korean coastal waters: Jinhae Bay case study. *Front. Mar. Sci.* 6, 359. doi: 10.3389/fmars.2019.00359

Zhao, M., and Zhang, S. (2022). The influence of shellfish farming on sedimentary organic carbon mineralization: A case study in a coastal scallop farming area of Yantai, China. *Mar. pollut. Bull.* 182, 113941. doi: 10.1016/j.marpolbul.2022.113941

Zhou, Y., Yang, H., Zhang, T., Liu, S., Zhang, S., and Liu, Q. (2006). Influence of filtering and biodeposition by the cultured scallop *Chlamys farreri* on benthic-pelagic coupling in a eutrophic bay in China. *Mar. Ecol. Prog. Ser.* 317, 127–141. doi: 10.3354/meps317127

Zúñiga, D., Castro, C. G., Aguiar, E., Labarta, U., Figueiras, F. G., and Fernández-reiriz, M. J. (2014). Biodeposit contribution to natural sedimentation in a suspended *Mytilus galloprovincialis* Lmk mussel farm in a Galician Ría (NW Iberian Peninsula). *Aquaculture* 432, 311–320. doi: 10.1016/j.aquaculture.2014.05.026